

## Brief Report

# Tumor Cells Genetically Labeled with GFP in the Nucleus and RFP in the Cytoplasm for Imaging Cellular Dynamics

Ping Jiang<sup>1</sup>

Kensuke Yamauchi<sup>1,2</sup>

Meng Yang<sup>1</sup>

Kazuhiro Tsuji<sup>1,2</sup>

Mingxu Xu<sup>1</sup>

Anirban Maitra<sup>3</sup>

Michael Bouvet<sup>2</sup>

Robert M. Hoffman<sup>1,2,\*</sup>

<sup>1</sup>AntiCancer, Inc.; San Diego, California USA

<sup>2</sup>Department of Surgery; University of California; San Diego, California USA

<sup>3</sup>Johns Hopkins University School of Medicine; Baltimore, Maryland USA

\*Correspondence to: Robert M. Hoffman, Ph.D.; 7917 Ostraw Street; AntiCancer, Inc., San Diego, California 92111 USA, Tel: 858.654.2555, Fax: 858.268.4175; Email: all@anticancer.com

Original manuscript submitted: 03/13/06

Manuscript accepted: 04/11/06

Previously published online as a *Cell Cycle* E-publication:

<http://www.landesbioscience.com/journals/cc/abstract.php?id=2795>

## KEY WORDS

GFP, RFP, double-labeled cells, nuclear-cytoplasmic dynamics, in vivo imaging

## ABBREVIATIONS

GFP green fluorescent protein  
RFP red fluorescent protein  
LLC Lewis lung carcinoma

## ACKNOWLEDGEMENTS

Supported in part by grants CA099258, CA103563, and CA101600 from the National Cancer Institute (AntiCancer, Inc.) and NIH grant R21 CA109949-01 and American Cancer Society RSG-05-037-01-CCE (M. Bouvet).

## ABSTRACT

Dual-color fluorescent cells with one color fluorescent protein in the nucleus and another color fluorescent protein in the cytoplasm were genetically engineered. The dual-color cancer cells enable real-time nuclear-cytoplasmic dynamics to be visualized in living cells in vivo as well as in vitro. To obtain the dual-color cells, red fluorescent protein (RFP) was expressed in the cytoplasm of a series of human and rodent cancer cells, and green fluorescent protein (GFP) linked to histone H2B was expressed in the nucleus. Nuclear GFP expression enabled visualization of nuclear dynamics, whereas simultaneous cytoplasmic RFP expression enabled visualization of nuclear-cytoplasmic ratios as well as simultaneous cell and nuclear shape changes. Using the Olympus OV100 Whole-Mouse Imaging System, total sub-cellular dynamics can be visualized in the living dual-color cells in real time in the live mouse after cell injection. Highly elongated cancer cells and nuclei in narrow capillaries were visualized where both the nuclei and cytoplasm deform. Both cytoplasm and nuclei were visualized to undergo extreme deformation during extravasation with cytoplasmic processing exiting vessels first and nuclei following along these processes. The dual-color cells described here thus enable the sub-cellular dynamics of cancer cell trafficking to be imaged in the living animal.

## INTRODUCTION

To externally image and follow the natural course or impediment of tumor progression and metastasis, a strong signal, high specificity and sensitivity as well as high resolution are necessary. The *GFP* gene, cloned from the bioluminescent jellyfish *Aequorea Victoria*,<sup>1</sup> was chosen to satisfy these conditions because it has these properties for use as a cellular marker.<sup>2,3</sup> GFP cDNA encodes a 283-amino acid monomeric polypeptide with *Mr* 27,000<sup>4,5</sup> that requires no other proteins, substrates, or cofactors to fluoresce.<sup>6</sup> Gain-of-function bright mutants expressing the *GFP* gene have been generated by various techniques<sup>7-9</sup> and have been humanized for high expression and signal.<sup>10</sup> Red fluorescent proteins (RFP) from the *Discosoma* coral have similar features as well as the advantage of longer-wavelength emission.<sup>11-13</sup>

We have developed whole-body imaging of tumor growth and metastasis in mice by use of tumor cells expressing GFP or RFP.<sup>14</sup> Fluorescence imaging presents many new possibilities for in vivo imaging including real-time studies of tumor progression, metastasis, and drug-response evaluations. With these fluorescent tools, single cells from tumors and metastases can be imaged in live animals. GFP technology has also been used for real-time imaging and quantification of angiogenesis.<sup>14</sup>

The present study uses a fusion of histone H2B and GFP (H2B-GFP)<sup>15</sup> and RFP to differentially label the nucleus and cytoplasm, respectively, of cancer cells. This dual-color tagging strategy also enables real-time observation of nuclear-cytoplasmic dynamics in vivo, including dynamics of trafficking and extravasating cancer cells.

## METHODS AND MATERIALS

**RFP retrovirus production.**<sup>16</sup> The *Hind* III/*Not* I fragment from pDsRed2 (Clontech), containing the full-length RFP cDNA, was inserted into the *Hind* III/*Not* I site of pLNCX2 (Clontech) that has the neomycin resistance gene to establish the pLNCX2-DsRed2 plasmid. PT67 cells, at 70% confluence, were incubated with a precipitated mixture of LIPOFECTAMINE<sup>TM</sup> reagent (Life Technologies), and saturating amounts of pLNCX2-DsRed2 plasmid using similar methods described above for GFP vector production. For selection of a clone producing high amounts of a RFP retroviral vector

(PT67-DsRed2), the cells were cultured in the presence of 200–1,000  $\mu\text{g/ml}$  of G418 for seven days the same as for PT67-GFP.

#### Production of histone H2B-GFP vector.<sup>16</sup>

The histone *H2B* gene has no stop codon, thereby enabling the ligation of the *H2B* gene to the 5'-coding region of the *A. victoria GFP* gene (Clontech). The histone H2B-GFP fusion gene was then inserted at the *HindIII/ClaI* site of the pLHCX (Clontech) plasmid that has the hygromycin resistance gene. To establish a packaging cell clone producing high amounts of a histone H2B-GFP retroviral vector, the pLHCX histone H2B-GFP plasmid was transfected in PT67 cells using the same methods described above for PT67-DsRed2. The transfected cells were cultured in the presence of 200–400  $\mu\text{g/ml}$  hygromycin for 15 days to establish stable PT67 H2B-GFP packaging cells.

**Double RFP and histone H2B-GFP gene transduction of cancer cells.<sup>16</sup>** For RFP and H2B-GFP gene transduction, 70% confluent cancer cells are used. To establish dual-color cancer cells, clones of cancer cells expressing RFP in the cytoplasm were initially established. In brief, cancer cells were incubated with a 1:1 precipitated mixture of retroviral supernatants of PT67-RFP cells and RPMI 1640 (Mediatech, Inc., Herndon, VA) containing 10% FBS for 72 h. Fresh medium was replenished at this time. Cells were harvested with trypsin/EDTA 72 h post-transduction and subcultured at a ratio of 1:15 into selective medium, which contains 200  $\mu\text{g/ml}$  G418. The level of G418 was increased stepwise up to 800  $\mu\text{g/ml}$ . RFP cancer cells were isolated with cloning cylinders (Bel-Art Products, Pequannock, NJ) using trypsin/EDTA and amplified by conventional culture methods. For establishing dual-color cells, RFP cancer cells were then incubated with a 1:1 precipitated mixture of retroviral supernatants of PT67 H2B-GFP cells and culture medium. To select the double transformants, cells were incubated with hygromycin 72 h after transfection. The level of hygromycin was increased stepwise up to 400  $\mu\text{g/ml}$ .

**Fluorescent animal models.<sup>17</sup>** To visualize cell dynamics in vessels in live mice, cells were injected into the heart. Nude mice were anesthetized with a ketamine mixture (10  $\mu\text{L}$  ketamine HCl, 7.6  $\mu\text{L}$  xylazine, 2.4  $\mu\text{L}$  acepromazine maleate, and 10  $\mu\text{L}$  H<sub>2</sub>O) via s.c. injection. A total of 200  $\mu\text{L}$  of medium containing  $5 \times 10^6$  dual-color cancer cells were injected into the heart. To observe the shapes of the dual-color cells within the microvessels before arrest, the epigastric cranialis vein of the mouse was wired with a 6-0 suture (Ethicon Inc., Somerville, NJ) before cell injection. Immediately after injection, an arc-shaped incision was made in the abdominal skin, and then s.c. connective tissue was separated to free the skin flap without injuring the epigastric cranialis artery and vein. The skin flap was spread and fixed on a flat stand. The inside surface of the skin flap was directly observed under fluorescence microscopy. After making the skin flap, dual-color cancer cells were imaged immediately. During the interval between imaging, PBS (Irvine Scientific) was occasionally sprayed on the inside of the skin flap to keep the surface wet. The skin flap could be completely reversed.

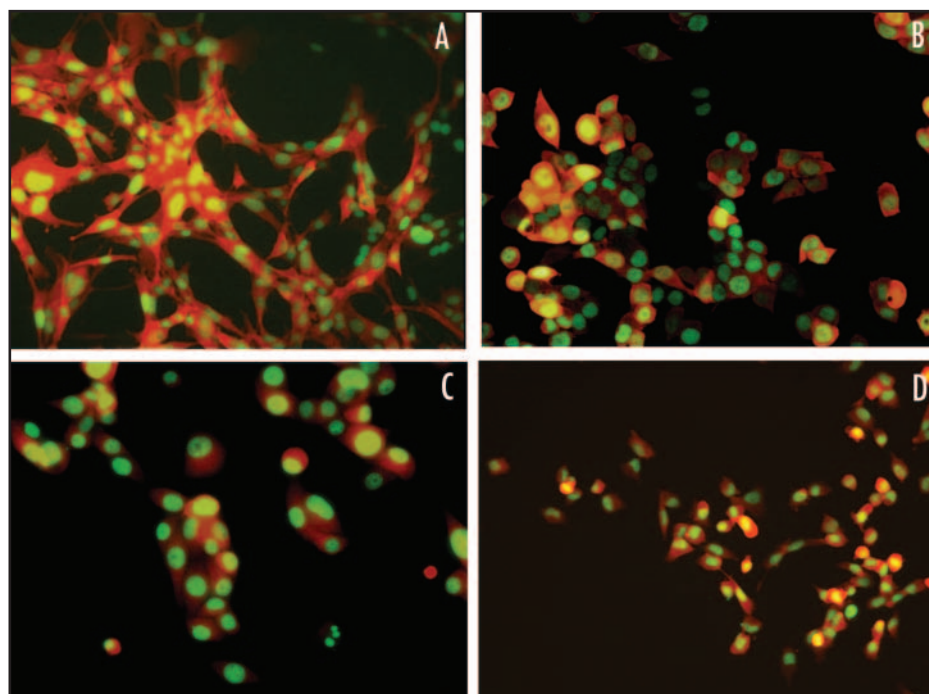


Figure 1. Stable high GFP- and RFP-expressing dual-color cancer cells in vitro. Cancer cells were initially transduced with RFP and the neomycin resistance gene. The cells were subsequently transduced with histone H2B-GFP and the hygromycin resistance gene. Double transformants were selected with G418 and hygromycin, and stable clones were established. (A) MMT mouse mammary cancer cell line; (B) HCT-116 human colon cancer cell line; (C) XIAP human pancreatic cancer cell line; (D) HT-1080 human fibrosarcoma cell line. See "Materials and Methods" for details. Bar = 50  $\mu\text{m}$ .

**Sub-cellular imaging in live animals.<sup>18</sup>** The Olympus OV100 Whole Mouse Imaging System (Olympus Corp., Tokyo, Japan), containing an MT-20 light source (Olympus Biosystems, Planegg, Germany) and DP70 CCD camera (Olympus Corp., Tokyo, Japan) was used. The optics of the OV100 fluorescence imaging system have been specially developed for macro as well as micro imaging with high light gathering capacity. The optics of the OV100 incorporate a unique combination of high numerical aperture and long working distance. Five individually optimized objective lenses, parcentered and parfocal, provide a 105-fold magnification range for seamless imaging of the entire body down to the single cell level without disturbing the animal. The OV100 has the lenses mounted on an automated turret with a magnification range of 1.6X to 16X and a field of view ranging from 6.9 mm–0.69 mm. The optics and anti-reflective coatings ensure optimal imaging of multiplexed fluorescent reporters in small animal models. High-resolution images were captured directly on a PC (Fujitsu Siemens, Munich, Germany). Images were processed for contrast and brightness and analyzed with the use of Paint Shop Pro 8 and Image ProPlus 3.1 software.

All animal studies were conducted in accordance with the principles and procedures outlined in the NIH Guide for the Care and Use of Laboratory Animals under assurance number A3873-1. Animals were kept in a barrier facility under HEPA filtration. Mice were fed with autoclaved laboratory rodent diet (Tecklad LM-485, Western Research Products, Orange, CA).

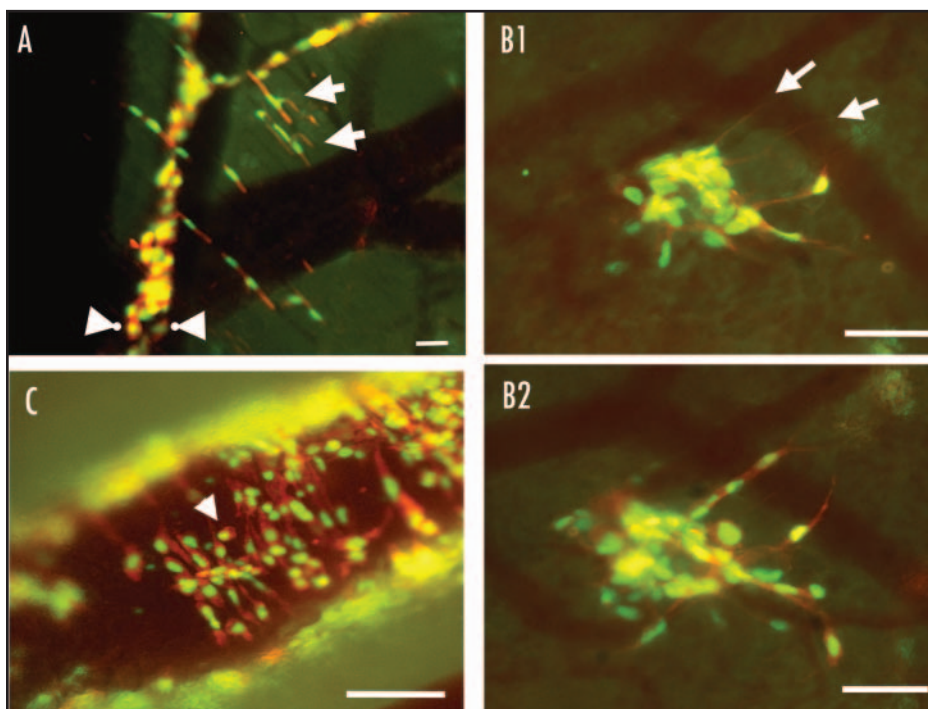


Figure 2. Imaging of dual-color cancer cells in live animals.<sup>17,18</sup> (A) Imaging dual-color cells in small and large blood vessels. The dual-color cancer cells in a large vessel are round and the nuclei oval. The cells and nuclei are elongated to fit in small-diameter capillaries. Bar = 50 μm. (B) Extravasating MMT cells. The cancer cells extend fine cytoplasmic projections into the host tissue at the onset of extravasation. The nuclei then migrate along the cytoplasmic projection until the whole cell is out of the vessel. Subsequently, the whole cell extravasates. Bar = 50 μm. (C) Proliferation of post-extravasation dual-color LLC cells on blood vessels. LLC cells are visualized to wind around a large vessel 120 h after injection. Most of the cells and nuclei are elongated with the major axes of the cells reaching approximately 100 μm. Mitotic cancer cells and premitotic round cancer cells whose nuclei are condensed are observed on the vessel wall. Bar = 100 μm. All in vivo images were acquired with the Olympus OV100 Whole Mouse Imaging System.

## RESULTS AND DISCUSSION

**Dual-color cancer cells in vitro.** Figure 1 shows the nuclear and cytoplasmic morphology examples of dual-color cell lines developed. Dual-color cell lines include the MMT mouse mammary cancer cell line (Fig. 1A); the HCT-116 human colon cancer cell line (Fig. 1B); the XIAP human pancreatic cancer cell line (Fig. 1C); and the HT-1080 human fibrosarcoma cell line (Fig. 1D). Note the unusual in vitro morphology of the MMT cells which grow very closely together and can only be distinguished as single cells by the dual-color labeling.

**Cell proliferation rates of parental and HT-1080-RFP-GFP-dual-color clones.** There was no difference in the proliferation rates of parental HT-1080 or HT-1080-dual-color clones determined in monolayer culture,<sup>16</sup> indicating that expression of GFP and/or RFP did not affect cell cycle progression.

**Imaging dual-color cancer cells in blood vessels in live mice.**<sup>17</sup> Real-time observations were made of nuclear-cytoplasmic deformation in capillaries of dual-color cancer cells compared to dual-color cancer cells in larger vessels. The cells were round and the nuclei were oval in large vessels. In capillaries, the cytoplasm and the nuclei were highly elongated (Fig. 2A).

**Imaging extravasation of dual-color cancer MMT cells in live mice.**<sup>18</sup> MMT cells extravasated by first extending cytoplasmic processes. After cytoplasmic processes were extended, the nuclei followed along the extension undergoing varying degrees of deformation to fit within the extended cytoplasmic protrusion. The whole cell eventually extravasated (Fig. 2B1, 2B2).

**Imaging extravasated dual-color Lewis lung carcinoma (LLC) cells surrounding and grow on vessels.**<sup>18</sup> Extravasated LLC cells were observed to surround a large vessel. Most of the cells were highly elongated, and the major axes of the cells stretched to approximately 100 μm (Fig. 2C). The cells and nuclei elongated in order to occupy as much area as possible on the vessel surface. Although the cancer cells, including their nuclei, elongated and extended their

cytoplasmic processes in order to surround the vessel, the elongated cells appear to round up before cell division, similar to attached cells in culture.

The dual-color cancer cells and the Olympus OV100 Whole-Mouse Imaging System, with macro-micro optics, used in the present study enable very high resolution of nuclear and cytoplasmic dynamics during intravascular cancer trafficking, extravasation and post-extravasation proliferation. The cell imaging techniques described here will enable future studies to further understand the mechanisms of cancer invasion and metastasis at the cellular and subcellular levels in vivo.

## References

- Prasher DC, Eckenrode VK, Ward WW, Prendergast FG, Cormier MJ. Primary structure of the *Aequorea victoria* green-fluorescent protein. *Gene* 1992; 111:229-33.
- Chalfie M, Tu Y, Euskirchen G, Ward WW, Prasher DC. Green fluorescent protein as a marker for gene expression. *Science* 1994; 263:802-5.
- Cheng L, Fu J, Tsukamoto A, Hawley RG. Use of green fluorescent protein variants to monitor gene transfer and expression in mammalian cells. *Nat Biotechnol* 1996; 14:606-9.
- Cody CW, Prasher DC, Westler WM, Prendergast FG, Ward WW. Chemical structure of the hexapeptide chromophore of the *Aequorea* green fluorescent protein. *Biochemistry* 1993; 32:1212-8.
- Yang F, Moss LG, Phillips GN Jr. The molecular structure of green fluorescent protein. *Nat Biotechnol* 1996; 14:1246-51.
- Morin J, Hastings J. Energy transfer in a bioluminescent system. *J Cell Physiol* 1971; 77:313-8.
- Cormack BF, Valdivia R, Falkow S. FACS-optimized mutants of the green fluorescent protein (*GFP*). *Gene* 1996; 173:33-8.
- Cramer A, Whitehorn EA, Tate E, Stemmer WP. Improved green fluorescent protein by molecular evolution using DNA shuffling. *Nat Biotechnol* 1996; 14:315-9.
- Delagrè S, Hawtin RE, Silva CM, Yang MM, Youvan DC. Red-shifted excitation mutants of the green fluorescent protein. *Biotechnology* 1995; 13:151-4.
- Heim R, Cubitt AB, Tsien RY. Improved green fluorescence. *Nature* 1995; 373:663-4.
- Zolotukhin S, Potter M, Hauswirth WW, Guy J, Muzyczka N. A 'humanized' green fluorescent protein cDNA adapted for high-level expression in mammalian cells. *J Virol* 1996; 70:4646-54.
- Gross LA, Baird GS, Hoffman RC, Baldrige KK, Tsien RY. The structure of the chromophore within DsRed, a red fluorescent protein from coral. *Proc Natl Acad Sci USA* 2000; 97:11990-5.
- Fradkov AF, Chen Y, Ding L, Barsova EV, Matz MV, Lukyanov SA. Novel fluorescent protein from *Discosoma* coral and its mutants possess a unique far-red fluorescence. *FEBS Lett* 2000; 479:127-30.

14. Hoffman RM. The multiple uses of fluorescent proteins to visualize cancer in vivo. *Nat Rev Cancer* 2005; 5:796-806.
15. Kanda T, Sullivan KF, Wahl GM. Histone-GFP fusion protein enables sensitive analysis of chromosome dynamics in living mammalian cells. *Curr Biol* 1998; 8:377-85.
16. Yamamoto N, Jiang P, Yang M, Xu M, Yamauchi K, Tsuchiya H, Tomita K, Wahl GM, Moossa AR, Hoffman RM. Cellular dynamics visualized in live cells in vitro and in vivo by differential dual-color nuclear-cytoplasmic fluorescent-protein expression. *Cancer Res* 2004; 64:4251-6.
17. Yamauchi K, Yang M, Jiang P, Yamamoto N, Xu M, Amoh Y, Tsuji K, Bouvet M, Tsuchiya H, Tomita K, Moossa AR, Hoffman RM. Real-time in vivo dual-color imaging of intracapillary cancer cell and nucleus deformation and migration. *Cancer Res* 2005; 65:4246-52.
18. Yamauchi K, Yang M, Jiang P, Xu M, Yamamoto N, Tsuchiya H, Tomita K, Moossa AR, Bouvet M, Hoffman RM. Development of real-time subcellular dynamic multicolor imaging of cancer-cell trafficking in live mice with a variable-magnification whole-mouse imaging system. *Cancer Res* 2006; 66:4208-14.